4-8-2010

Spatially Distributed Tactile Feedback for Kinesthetic Motion Guidance

Pulkit Kapur
University of Pennsylvania, pkapur@seas.upenn.edu

Mallory Jensen
University of Pennsylvania, jensenma@seas.upenn.edu

Laurel J. Buxbaum
Moss Rehabilitation Research Institute

Steven A. Jax
Moss Rehabilitation Research Institute

Katherine J. Kuchenbecker
University of Pennsylvania, kuchenbe@seas.upenn.edu

Spatially Distributed Tactile Feedback for Kinesthetic Motion Guidance

Abstract
Apraxic stroke patients need to perform repetitive arm movements to regain motor functionality, but they struggle to process the visual feedback provided by typical virtual rehabilitation systems. Instead, we imagine a low cost sleeve that can measure the movement of the upper limb and provide tactile feedback at key locations. The feedback provided by the tactors should guide the patient through a series of desired movements by allowing him or her to feel limb configuration errors at each instant in time. After discussing the relevant motion capture and actuator options, this paper describes the design and programming of our current prototype, a wearable tactile interface that uses magnetic motion tracking and shaftless eccentric mass motors. The sensors and actuators are attached to the sleeve of an athletic shirt with novel plastic caps, which also help focus the vibration on the user's skin. We connect the motors in current drive for improved performance, and we present a full parametric model for their in situ dynamic response (acceleration output given current input).

Disciplines
Engineering | Mechanical Engineering

Comments
Suggested Citation:
Kapur, Pulkit, Mallory Jensen, Laurel J. Buxbaum, Steven A. Jax and Katherine J. Kuchenbecker. (2010). *Spatially distributed tactile feedback for kinesthetic motion guidance.* Haptics Symposium 2010. Waltham, Massachusetts. March 25-26, 2010.

Spatially Distributed Tactile Feedback for Kinesthetic Motion Guidance

Pulkit Kapur*, Mallory Jensen*, Laurel J. Buxbaum§, Steven A. Jax§ and Katherine J. Kuchenbecker*

*Haptics Group, GRASP Laboratory
University of Pennsylvania, USA
{pkapur,jensenma,kuchenbe}@seas.upenn.edu

§Cognition and Action Laboratory
Moss Rehabilitation Research Institute
{lbuxbaum,jaxs}@einstein.edu

ABSTRACT

Apraxic stroke patients need to perform repetitive arm movements to regain motor functionality, but they struggle to process the visual feedback provided by typical virtual rehabilitation systems. Instead, we imagine a low cost sleeve that can measure the movement of the upper limb and provide tactile feedback at key locations. The feedback provided by the tactors should guide the patient through a series of desired movements by allowing him or her to feel limb configuration errors at each instant in time. After discussing the relevant motion capture and actuator options, this paper describes the design and programming of our current prototype, a wearable tactile interface that uses magnetic motion tracking and shaftless eccentric mass motors. The sensors and actuators are attached to the sleeve of an athletic shirt with novel plastic caps, which also help focus the vibration on the user's skin. We connect the motors in current drive for improved performance, and we present a full parametric model for their in situ dynamic response (acceleration output given current input).

1 INTRODUCTION

More than 780,000 Americans suffer a stroke each year, and approximately 80% of these individuals survive and require rehabilitation to regain motor functionality [1]. Many of these patients are subsequently afflicted by ideomotor limb apraxia, a motor control condition that hinders one's ability to carry out skilled upper-limb movements, like those required for the activities of daily living [5]. Specifically, deficits in motor planning often prevent apraxic patients from executing a desired motion command, even though they comprehend the goal and have the sensory capabilities required to do the task. Fortunately, rehabilitation therapy has been shown to help improve these patients' capabilities, though the optimal treatment method is not yet known [5].

One promising new approach for stroke rehabilitation is virtual reality (VR). This technology allows the user to interact with virtual three-dimensional environments generated by a computer, which provides a treatment platform that is both flexible and consistent. VR-augmented rehabilitation tasks often involve repeatedly imitating desired movements that are portrayed graphically. One substantive benefit to this approach is that patient motion can be recorded, analyzed, and tracked over time. However, existing virtual reality systems rely primarily on visual feedback, which apraxic patients struggle to interpret.

We believe that carefully designed tactile cues have the potential to enhance VR-based rehabilitation for apraxic patients. Everyday experience shows that the sense of touch is indispensable for many routine tasks, working in close coordination with vision, hearing, and the motor control system. Specifically, the skin provides one with a large area for receiving diverse tactile cues, and it enables one to localize and recognize individual stimuli quite easily, even when one's limbs are moving. We thus hypothesize that real-time tactile feedback applied to the working arm could help apraxic patients understand the desired arm motions and correct motion errors during rehabilitation.

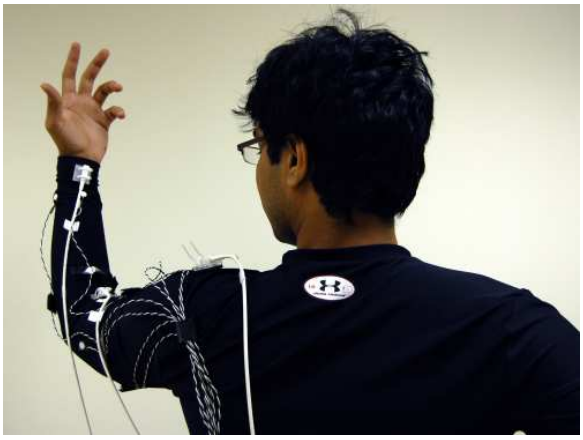

(a) User wearing the tactile interface sleeve

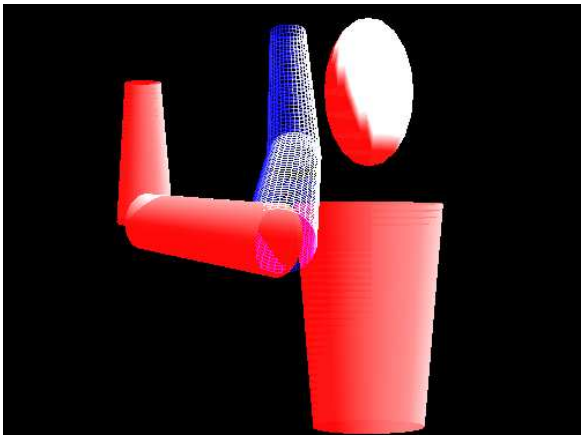

(b) Graphical rendering of the user's arm pose (solid red) and the desired configuration (wireframe blue).

Figure 1: The user wears the tactile sleeve, which is embedded with motion capture sensors and tactile actuators, and sees his or her arm pose on a screen.

Even as more research is being done to develop effective rehabilitation devices, current devices are priced prohibitively high for most clinics. This large cost prevents a large section of society from obtaining access to new therapeutic methods. To serve apraxic patients and overcome cost limitations, we have developed a prototype for a low cost VR-based haptic interface for upper limb rehabilitation, as seen in Figure 1.

In the following sections we present a background on modern rehabilitation technologies and tactile feedback for motion guidance, followed by a discussion of our overall system vision. Next we

IEEE Haptics Symposium 2010
25 - 26 March, Waltham, Massachusetts, USA
978-1-4244-6822-5/10/$26.00 ©2010 IEEE

explain the development of our current prototype, a wearable tactile interface for upper-limb rehabilitation tasks. We then detail our tactile feedback algorithms for the upper arm and the forearm, followed by development of a dynamic model of our tactile actuator. We conclude with the summary of this paper and a discussion of our plans for the future.

2 BACKGROUND

Traditional rehabilitation therapy involves repeating specified arm motions, with a therapist providing hand-over-hand skilled guidance (shaping) to assist the affected arm in performing functional tasks. These training methods are work-intensive for the therapist and can become boring and laborious for the patient, thus presenting the need to develop alternative therapy methods. Newer rehabilitation therapy benefits from the use of virtual reality and assistive robotic arms. These technologies permit the delivery of enhanced feedback and guided practice as well as the option to record user performance for evaluation. Representative examples of these techniques are discussed in the following sections.

2.1 Robotic Rehabilitation

Robotic rehabilitation systems consist of a VR environment in which patients repeatedly imitate desired motions with the aid of a powered linkage or an exoskeleton. Among the commonly used therapy robots is the MIT-Manus, a planar SCARA module allowing two-dimensional motion [12]. It is back drivable with low inertia and friction, allowing for low impedance and minimal encumbrance of the patient. The force and position sensors on the planar linkage allow input to the impedance controller. A three degree of freedom (d.o.f.) module can be mounted on the end of the planar module to provide additional wrist motions in three active d.o.f. Visual feedback is provided with an overhead display monitor. Advantages of robotic rehabilitation over conventional therapy include increased intensity, more repetitions, better patient engagement, enhanced motor learning via additional visual stimuli, outstanding standardization of movements within and between sessions, and the ability to track patient response longitudinally over time. A more detailed and comparative study of other such robotic-rehabilitation devices is provided in [17].

Despite their advantages, most current robotic rehabilitation devices are expensive, bulky, have a large footprint, and have limited flexibility and workspace. Morever, robotic devices change the dynamics of the human limb, which may hinder the patient's ability to transfer training experiences to everyday living. A recent analysis of ten studies comprising 218 patients concluded that upper extremity robotic treatment improved motor recovery as compared with traditional rehabilitation therapy. However no differences were found for performance-based measures such as the activities of daily living [13].

2.2 Tactile Feedback for Motion Guidance

Traditionally, researchers have used two dimensional tactor arrays as a means of displaying the spatial distribution of information in a stationary location. These are equivalent in the domain of programmable visual displays to a two dimensional rasterized image with a fixed pixel density. A great deal of information can be conveyed through this approach (often on the torso and more recently on the tongue), particularly in sensory substitution for visually impaired individuals [2]. Unfortunately, the learning curve is steep and processing is slow because the skin is not naturally adapted to receive this type of information.

More recently, researchers have used skin stretch (shear forces) as a means of communicating information to subjects. In contrast to the rasterized feedback discussed previously, these skin stretch devices can be understood as tactile vectors: each stimulus conveys a magnitude and a direction. For example Gleeson et al. used lateral skin stretch on the fingertip to provide two d.o.f. directional cues [9], and Bark et al. used rotational skin stretch on the arm to provide feedback regarding the movement of a virtual object [3]. Though promising, present versions of these devices are bulky, have a number of moving parts, and can cause discomfort if the skin is stretched beyond a threshold.

Another method for tactilely conveying a magnitude and a direction is to position an array of actuators across the user's body, rather than on just a single region of their skin. One can then use each actuator's location to signify an intended direction of motion, while magnitude can be transmitted via the intensity of the tactile stimulation at that point. Rather than choosing an arbitrary relationship between tactor locations and motion directions, we believe the most intuitive mapping for such feedback builds on an analogy to contact or proximity, such that the user is encouraged to move his or her limb away from the point where tactile feedback is felt.

One recent implementation of this spatially distributed contact feedback approach was done by Bloomfield and Badler [4], who created a tactile sleeve embedded with vibrotactile actuators and optical motion-tracking markers. Subjects reached within 3D virtual puzzles while trying to avoid collisions with the walls. They received spatial tactile collision feedback, visual feedback, both of these, or none of these. The tactors (eccentric-mass DC motors) were driven at three different levels: off for no contact, on at fixed frequency and amplitude for medium-depth collisions, and pulsing for deep collisions. Despite this simple tactor feedback algorithm and the fact that users could not adequately distinguish the second and third types of tactile feedback, the associated human-subject experiment showed a significant collision avoidance benefit to the tactile feedback over the other three tested modalities. Similar studies on the use of vibrotactile feedback for spatial contact feedback in an immersive virtual environment were shown in [22] and [15]. More recently, Tadakuma and Howe [20] used RC-servo paddles to provide contact location feedback on the arm for whole-arm telemanipulation. Results showed that this novel tactile feedback enabled subjects to consistently grasp the virtual object being manipulated, even in the absence of visual information.

In related work, Cassinelli, Reynolds and Ishikawa [6] used distributed tactile feedback to augment a user's spatial awareness. The "Haptic Radar" consists of eight modules (self-contained pairs of proximity sensors and vibrotactile actuators) located in a band around the user's head. The tactors were each programmed to vibrate in proportion to local object proximity. The subject was blindfolded, and his or her ability to react to unseen approaching objects was directly assessed. Without being told how the device operates, only knowing that they were supposed to avoid object contact, subjects managed to correctly react to (move away from) stimuli in over 85% of the trials. This result again supports the use of graded distributed tactile feedback for motion guidance.

Several recent visual VR systems have capitalized on the concept of imitating a virtual teacher who performs movements many times over within the context of virtual functional tasks (e.g., wiping a tabletop or lifting a cup to the mouth) [10, 7]. To facilitate movement matching, a pre-recorded trajectory of the correct movement is displayed alongside the real-time trajectory of the patient's own movement. The degree of match may also be quantified to provide augmented feedback in the form of a score or other verbal feedback. To our knowledge, the only implementation of this concept to include tactile feedback is the work of Lieberman and Breazeal [14]. The Tactile Interaction for Kinesthetic Learning (TIKL) system provides vibrotactile feedback on five d.o.f. of the arm for training students to mimic motions demonstrated by an expert. Subjects wear a suit embedded with Tactaid voice coil vibrotactile actuators (www.tactaid.com/skinstimulator.html), and they try to mimic motions performed by the teacher while being tracked

by a Vicon optical motion capture system (www.vicon.com). When the subject deviates from the target trajectory, vibrotactile feedback proportional to the amount of error is provided. Feedback on forearm pronation/supination and shoulder internal/external rotation is accomplished using the sensory saltation effect [8]: a sequence of successive tactor activations is generated around the wrist at a fixed rate of 9 Hz. The sequence is either clockwise or anti-clockwise depending on the sign of error for the joint. The authors reported 15% gain in subject performance and 7% increase in learning with the addition of tactile feedback over subjects with only visual feedback. However this system uses an expensive Vicon motion capture system, which suffers from problems of marker occlusion and large workspace requirements, making it unsuitable for clinical environments. Furthermore, the results for correcting rotational errors using the sensory saltation effect did not show a statistically significant benefit.

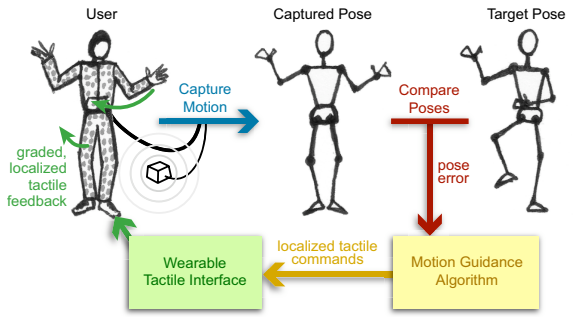

Figure 2: Envisioned system for kinesthetic motion guidance via spatially distributed tactile feedback

3 System Overview and Design Options

Inspired by the idea of using spatially distributed tactile feedback for motion guidance, we aim to create a new low-cost rehabilitation system that measures the patient's arm movements in real time and uses a combination of graphical and tactile feedback to guide him or her through a set of motions chosen by the therapist. Figure 2 shows of our envisioned system. This approach could aid in the rehabilitation of stroke patients suffering from ideomotor limb apraxia, which causes difficulty at imitating motions that are visually demonstrated.

The user of the envisioned system wears a full-body suit that is densely embedded with tactile actuators. He or she views the posture or motion to master on a screen and attempts to move his or her body to match. The movements of all the body segments are tracked through a motion capture system, displayed on the screen, and compared with the target body configuration in real time. When the user deviates more than a small amount from this target, tactors on the associated limb segment provide feedback, helping the user know how to translate or rotate that part of his or her body toward the correct configuration. The vibration feedback from each tactor is intended to be a repulsive cue to push the user away. This is similar to the light touch of a therapist guiding the patient to target configurations in a traditional rehabilitation paradigm.

The first step in developing our envisioned system is to select a suitable motion capture system, which will obtain the user's current joint angles in real time. Ideally the motion capture system should minimally encumber the user, achieve high position sensing accuracy, and be robust to interference from tactors and other elements in the vicinity [21]. Optical motion capture systems typically consist of a set of cameras in the surroundings and optical markers on the subject. The motion is captured when light emitted or reflected by the markers is sensed by the cameras. Triangulation and multi-base correlation methods are then used to estimate the position and orientation of the markers with respect to the cameras. The system generally outputs quaternion or euler angle data for each limb with respect to ground. This data can then be converted to joint angle data using simple transformation rules. However, a major disadvantage of optical motion capture systems is marker occlusion, which causes ambiguity in the location and orientation of limbs and joints in space. Also, optical motion capture systems require large capture volumes making them unsuitable for rehabilitation environments.

Inertial motion capture systems, on the other hand, use gyroscopes, accelerometers, and magnetometers to estimate the position and orientation of a limb in space. A typical commercial inertial measurement unit (IMU) consists of three orthogonal gyroscopes to estimate the yaw, pitch and roll angles, and three orthogonal accelerometers. The acceleration vector measured by the accelerometers in the body frame is converted to the fixed frame using the rotational matrix as determined by the gyroscopes. This acceleration vector is then gravity compensated and double integrated to get the position of the body with respect to the fixed frame. A drawback of this approach is the drift in position output obtained from accelerometer signals. A small bias error in the acceleration signal is integrated and amplified to a large error in position within a small time. Similarly, any error in gyroscope output produces a large error in the gravity compensation on the accelerometers, thus causing errors in accurately estimating the orientation and position of the body.

Magnetic motion capture systems utilize three-axis generation and sensing of quasi-static magnetic dipole fields to measure the full position and orientation of the sensor relative to the source [16]. The major advantages of magnetic tracking system are that the sensors are small, they have no line of sight requirements, and a single source unit can be used to track four to eight sensors. However, they are susceptible to interference from ferro-magnetic and conductive metals in the vicinity. If these concerns can be addressed magnetic motion capture is an excellent option for the envisioned application.

The second step in developing our proposed system is to pick tactile actuators. There are a variety of actuation techniques we can employ to deliver spatially localized tactile feedback on the user's skin. Many common tactile actuators produce vibrations that are sensed by the mechanoreceptors located in the skin. Other tactile actuators produce pain, stretch, pressure, or thermal effects. Tactor technologies range from more complex and expensive electro-active polymer actutators, piezoelectric bending elements, solenoids, and voice coil actuators to the simple and inexpensive rotating eccentric mass motors. Among these, voice coil actuators, which have an oscillating coil suspended in a magnetic field, seem promising because of their ability to generate a rich variety of tactile sensations. Tactors that contact the skin intermittently and impart tapping sensations similar to real world contact are also an interesting avenue to explore.

In our initial work on this project, we created and presented a hands-on demonstration of a low cost tactile feedback system for motion guidance on elbow flexion/extension and forearm pronation/supination degrees of freedom [11]. Users held the handle of a two d.o.f. passive exoskeleton (fitted with potentiometers) and were provided tactile cues through a wrist band (embedded with shaftless eccentric mass vibration actuators). Graphical feedback was provided about the user's current forearm configuration and the desired pose on a screen. This early prototype and the user feedback it inspired have helped inform the development of our current system.

4 Current Prototype

To investigate the merits of our envisioned approach to stroke rehabilitation, we have created a prototype sleeve system. This wearable tactile interface has three main objectives. It should be com-

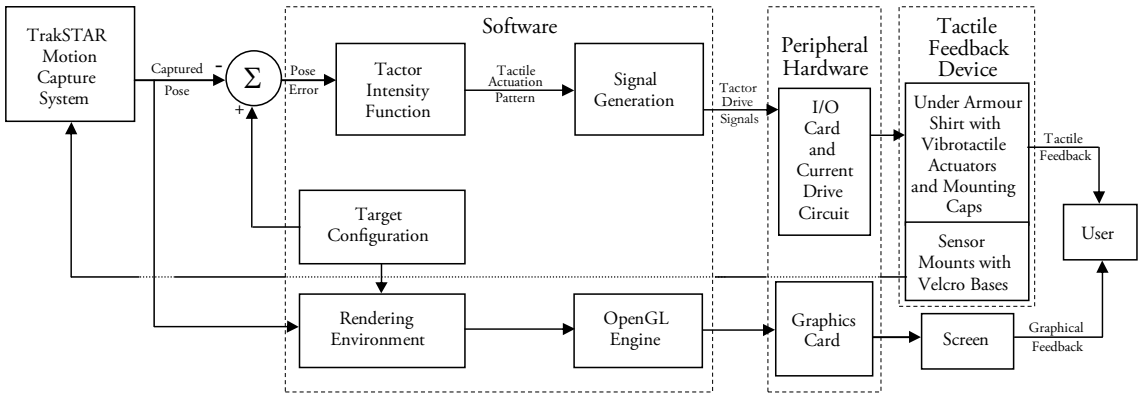

Figure 3: Block diagram of system configuration

fortable and easy to wear without encumbering the user, it should continually and reliably measure the configuration of the user's arm in space, and it should provide intuitive tactile cues to guide the user into target configurations. Our current prototype uses vibrotactile feedback to guide the user's arm to target poses composed of four degrees of freedom: elbow flexion/extension, shoulder inward/outward rotation, shoulder flexion/extension, and shoulder abduction/adduction. The basis of the interface is a long-sleeved Under Armour athletic shirt, with motion capture sensors and tactile actuators placed on the sleeve. A stretchable fabric was chosen to create a tight fit. This ensures that the actuators are close to the skin for good tactile sensation, and it accounts for small variations in size among users. We use Under Armour shirts in men's medium and men's large sizes to fit a broad section of users. Figure 3 depicts the block diagram of the entire system, and the following subsections describe the motion capture and actuation technologies used in our current prototype.

4.1 Motion Capture

The motion of the user's arm is measured with an electromagnetic motion tracking system (TrakSTAR, Ascension Technology Inc.) Three sensors were used in this system, as shown in Figure 4. Sensor one is on the forearm near the wrist, sensor two is on the upper arm near the elbow, and sensor three is mounted on the clavicle next to the shoulder joint. Each sensor has three orthogonal coils that provide six d.o.f. (both position and orientation) information of the sensor with respect to a stationary field-generating transmitter. Each sensor is 19×8×8 mm and has an update rate of 240 Hz. The transmitter has a maximum range of 78 centimeters. The system has a static positional accuracy of 1.4 mm (RMS) and orientation accuracy of 0.5 degrees (RMS). As seen in Figure 1(a), the sensors are mounted on small acrylic pads and secured via zip ties. Velcro hooks (rough side) are attached underneath the pads that join with velcro loops (soft side) sewn onto the sleeve. Small velcro patches are also attached to the sensor cable to route it securely along the user's arm.

The orientation output for each sensor is in the form of a sequence of Euler angle rotations of the sensor with respect to the transmitter reference frame. This rotational sequence is defined as an azimuth (about the reference frame's Z axis), then an elevation (about the rotated frame's new Y axis), and finally a roll (about the new X axis), in that order. The process of calculating arm joint angles from raw sensor data includes an initial calibration routine and subsequent measurement steps.

The calibration routine is required to account for variations in sensor mounting on the user's arm. In this step, the user is asked to mimic a calibration pose (stretching the arm straight out, perpendicular to the coronal plane) and the orientation of each sensor is

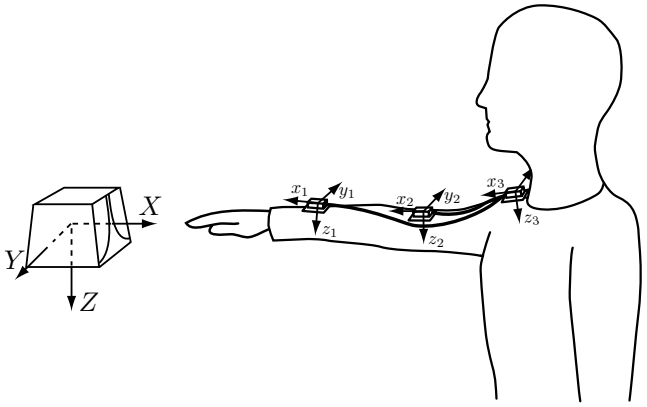

Figure 4: Pose used for calibration of motion capture system

recorded. As is evident from Figure 4, each sensor's x-and y-axes are approximately aligned with the negative X-and Y-axes of the transmitter, respectively, and both the sensor's and transmitter's Z-axes are approximately aligned. This means that the sensor's frame of reference is rotated by 180 degrees about the Z-axis, resulting in 180 degrees azimuth and 0 degree elevation and roll. Any difference in the recorded calibration data from this expected output is corrected by rotating the sensor's frame by the difference. This is done using the inbuilt angle align routine in the TrakSTAR's API. The calibration routine also uses the position information of each sensor to calculate the user's upper arm and forearm lengths, which are passed as input to the graphical rendering algorithm.

Next, the system must compute joint angles at each step in time from the calibrated position and orientation information. This is done in the following manner, where $\vec{r}_y^x$ denotes the position vector x in the frame of y:

- Elbow flexion/extension angle is the angle between the x-axis of sensor 2 and the x-axis of sensor 1.

$$\vec{r_{1_A}^x} = R_A^1 \vec{r_1^x} \tag{1}$$

$$\vec{r_{2_A}^x} = R_A^2 \vec{r_2^x} \tag{2}$$

$$\theta = \arccos(\vec{r_{2_A}^x}, \vec{r_{1_A}^x}) / |\vec{r_{1_A}^x}||\vec{r_{2_A}^x}| \tag{3}$$

- Forearm pronation/supination angle is the angle between the y-axis of sensor 2 and the y-axis of sensor 1.

$$\vec{r_{1_A}^y} = R_A^1 \vec{r_1^y} \tag{4}$$

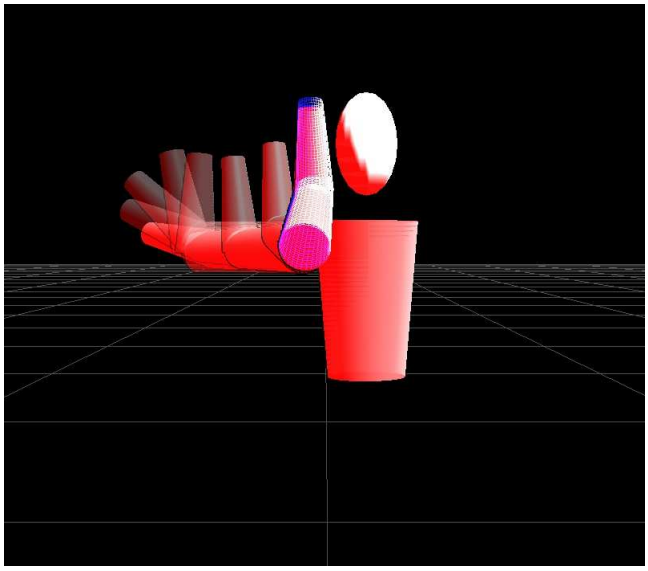

Figure 5: A time lapse view of the user moving his or her arm toward the target configuration

$$\vec{r_{2_A}^{y}} = R_A^2 \vec{r_2^{y}} \tag{5}$$

$$\phi = \arccos(\vec{r_{2_A}^{y}}, \vec{r_{1_A}^{y}})/|\vec{r_{1_A}^{y}}||\vec{r_{2_A}^{y}}| \tag{6}$$

- The shoulder joint angles are found by first calculating the rotational matrix of the upper arm with respect to the torso, i.e., R_3^2 where,

$$R_3^2 = R_A^2[R_A^3]^T \tag{7}$$

  Computing the Euler angles of this rotation matrix gives us the angles of the shoulder joint with respect to the torso. We follow the conversion procedure detailed in [19], taking into account gimbal lock.

The joint angles calculated above are used to display the user's current arm configuration on a computer screen using OpenGL, as seen in Figure 5. We model the user's upper arm and forearm as solid red tapered cylinders, and the target pose is depicted as a pair of blue wire frame cylinders. A stationary head and torso are added to the graphics for completeness. When the user achieves the target pose within a pre-defined angular tolerance, the color of the two cylindrical links turns from red to blue.

4.2 Tactile Actuation

Our choice of tactile actuation methods was based on several considerations. Key among them were the richness of the tactile stimulus, choice of a variety of drive signals, fast response time, small form factor, ease of availability, ability to modulate the intensity of stimulus, and low cost. We experimented with several alternatives for providing the desired feedback to the user. First we tested C2 tactors, manufactured by Engineering Acoustics, Inc. (www.eaiinfo.com). These are voice coil actuators with a 30 mm diameter, and they cost approximately $200 each. Each tactor incorporates a moving contactor that is lightly preloaded against the skin. This circular piece gently presses on the user's skin and is capable of delivering a variety of sensations because it can be driven independently with waveforms of different frequencies, amplitudes, and/or shapes. Although C2 tactors provide a rich array of vibrotactile sensations, their high cost is a detriment to the design of an affordable rehabilitation system, and their size is not ideal. Keeping this in mind, we tried 25 mm diameter sub-woofer speakers from

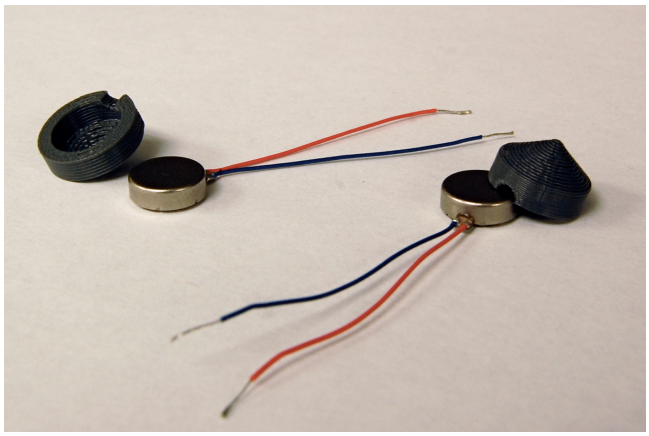

Figure 6: Shaftless eccentric mass vibration actuators with plastic caps used for mounting

GE bass-boost headphones. These actuators cost approximately $8 each and are ideal for a low cost system. However, like the C2 tactors, the form factor of the sub-woofer speakers was not suitable for mounting the tactors on the wrist, so we sought other options.

Next, we experimented with solenoids mounted normal to the skin's surface to provide an intermittent contact sensation. However, the low output-force-to-size ratio makes solenoids unsuitable for this application. In order to achieve the dual requirements of low cost and small size, shaftless eccentric mass vibration actuators were a suitable choice. These tactors are 10 mm in diameter and are economically priced at only a few dollars each. However the disadvantages of these tactors are that they require high spin-up times to reach desired amplitudes and that their output amplitude and frequency are linked togeather by the rotational dynamics of the eccentric mass. In order to localize the tactile sensation on the skin we designed and used custom-built plastic caps that have a tapered conical head. A similar tip was used in previous work [18] to improve localization of vibrotactile stimuli.

Eight shaftless eccentric mass motors are mounted on the sleeve via plastic caps as shown in Figure 6. The cap is located under the sleeve, while the tactor is placed on top of the sleeve. The two parts snap togeather over the fabric for an interference fit. Thus, in addition to helping focus the vibrations, the caps serve as an easily movable mechanical connector.

These tactors are driven using a linear current amplifier circuit, which controls the amount of current passing through the motor at each instant. This is in contrast to the voltage drive circuit that is usually used to drive these devices. The current drive masks the motor's electrical dynamics, giving the system more direct control over mechanical behavior. The current sent to each actuator directly controls the torque, which helps to speed up the transient response of the motor. These considerations are discussed more in Section 6.

5 Tactile Feedback Algorithm

During operation, our tactile feedback system is commanded with a well-defined desired arm configuration. This desired configuration may be either a static pose or a step along a recorded motion trajectory. In designing the tactile feedback algorithm, we must establish a feedback policy that makes the subject want to move towards the target. There are two aspects to the design of this tactile gradient: the choice of which tactors to employ (a negative spatial cue) and the intensity with which each tactor should each be activated (an error magnitude cue). We chose to use tactile feedback derived from joint angle errors to guide the subject to target arm configurations, as we believe this may be an intuitive motion domain. This choice

is similar to Lieberman and Breazeal [14] and is in contrast to the Cartesian collision paradigm chosen by Bloomfield and Badler [4]. For each joint we define an angular tolerance, $\theta_{Tolerance}$, which is used to determine whether the current pose is close enough to the goal. This angular tolerance can be adjusted for different users to make the task easier or more difficult.

The first step is to determine which actuators to turn on to guide the user towards the target. We consider vibrotactile feedback provided by the tactors as a negative spatial cue which is repulsive and seeks to push the user away. The chosen tactors provide cues that make the user move in a direction that decreases the angular error. For example, a need for elbow extension is spatially signaled by tactor activation on the forearm surface that is currently facing the upper arm; this elbow angle error can be naturally corrected by moving away from the negative tactile stimulus until it disappears.

The second step is to determine the intensity level for each selected tactor. The tactors may be turned on in a binary fashion, i.e., either completely on or off, or their amplitude may be a function of a system parameter, such as the desired angle or the angular error. We choose to grade the tactile signals such that their salience corresponds to the magnitude of the error. This not only reinforces the preferred direction of motion but also helps the user to dynamically determine which body part to attend to. Mathematically, this can be represented as follows:

$$i = \begin{cases} 0 & if\ |\theta_{Error}| \leq \theta_{Tolerance} \\ k_p(|\theta_{Error}|) & if\ |\theta_{Error}| > \theta_{Tolerance} \end{cases} \quad (8)$$

where k_p is a proportionality constant in amps per degree and i is the current command to the linear current amplifier.

Our present sleeve prototype provides feedback for four degrees of freedom of the human arm: elbow flexion/extension, shoulder inward/outward rotation, shoulder adduction/abduction and shoulder flexion/extension. Among these, feedback for elbow flexion/extension and inward/outward shoulder rotational errors is provided by using four tactors located on the wrist, while feedback for shoulder flexion/extension and shoulder abduction/adduction errors is provided by using four tactors located on the upper arm near the elbow. We think of the applied stimuli as tactile joint torques that seek to reduce the angular error. It should be mentioned that the tactors are placed far from the joints being corrected to obtain the largest *moment arm* about the joint.

In our tactile feedback algorithms for elbow flexion/extension and shoulder inward/outward rotation, we define a variable ϕ which provides the spatial location of a tactor on the wrist at any instant, where

$$\phi_j = \theta_j + \psi(t) \quad (9)$$

where θ_j is the initial tactor location on the wrist and $\psi(t)$ is the forearm pronation/supination angle (which we measure but do not seek to guide).

The tactile feedback is computed using the following algorithm: if the angular error θ_{Error} is positive,

$$i_j = \begin{cases} -k_P(\cos\phi_i)(|\theta_{Error}|) & if\ \phi_j \leq 180\ and\ \phi_j > 0 \\ 0 & if\ \phi_i \leq 0\ and\ \phi_j > 180 \end{cases} \quad (10)$$

The opposite is true when θ_{Error} is negative. We can write a similar algorithm for tactors located on the upper arm.

6 Motor Dynamics and Analytical Modeling

In order to better control the accelerations produced by our eccentric mass motors, we have developed a dynamic model to predict the motor response to system commands. This Matlab model takes as inputs time and current commanded to the circuitry. In creating this simulation, we developed a simple mechanical model (Figure 7), determined this system's characteristic equations, measured

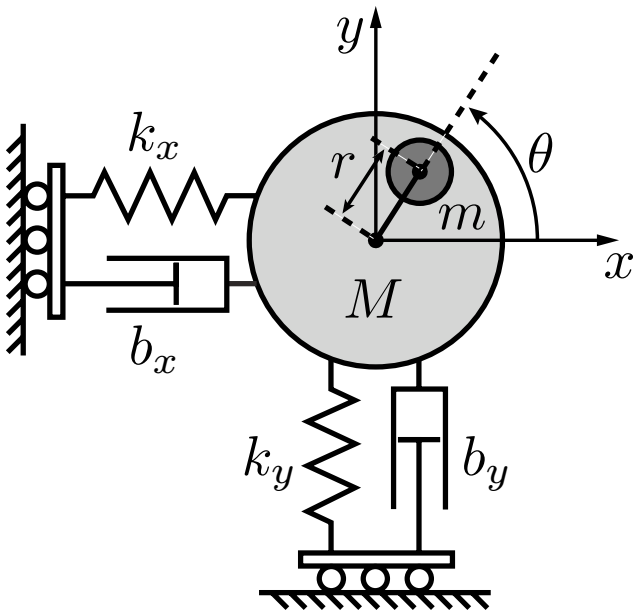

Figure 7: A simple parametric model for the mechanical dynamics of a shaftless eccentric mass motor.

required system parameters, and finally correlated the model to experimental data.

To write the equations representing our motor, we made several assumptions about the system. First, we assumed that the motor housing vibrates only in the plane of the skin and does not rotate; in other words, the vibration causes no normal forces and no in-plane torques on the user's skin. Second, we represented the skin and fabric surrounding the motor and its cap by a pair of linear springs and viscous dampers. Finally, the rotating element was approximated as a point mass on a massless string. Although we know its shape, a close examination of this piece will show that its mass is concentrated in a counterweight on its outer radius.

The six state variables for our motor model are eccentric mass angular position θ and velocity $\dot{\theta}$, horizontal motor housing position x and velocity $\dot{x}$, and vertical motor housing position y and velocity $\dot{y}$. The rotation of the eccentric mass is governed by the following equation:

$$mr^2\ddot{\theta} = k_t i - \tau_f \quad (11)$$

Here, m is the mass of the rotating part, r is its radial distance from the housing's center of mass, k_t is the motor's torque constant, and τ_f is the torque applied by friction. Next, we can write the force balance equations by tracking the displacement of the center of mass of the entire system:

$$(m+M)\ddot{x} = mr\ddot{\theta}\sin\theta + mr\dot{\theta}^2\cos\theta - k_x x - b_x\dot{x} \quad (12)$$

$$(m+M)\ddot{y} = mr\ddot{\theta}\cos\theta + mr\dot{\theta}^2\sin\theta - k_y y - b_y\dot{y} \quad (13)$$

Here, M is the combined mass of the motor housing and plastic cap, k_x and k_y are the horizontal and vertical stiffness of the skin and fabric surrounding the motor, and b_x and b_y are the horizontal and vertical damping of these materials.

In current drive, these three mechanical equations specify all of the dynamics required to predict the acceleration that the user will feel. We use the ode15s function in Matlab to simulate this six-state system over time. For a given current input over time, our script calculates, outputs, and plots the system's linear and angular positions, velocities, and accelerations over time.

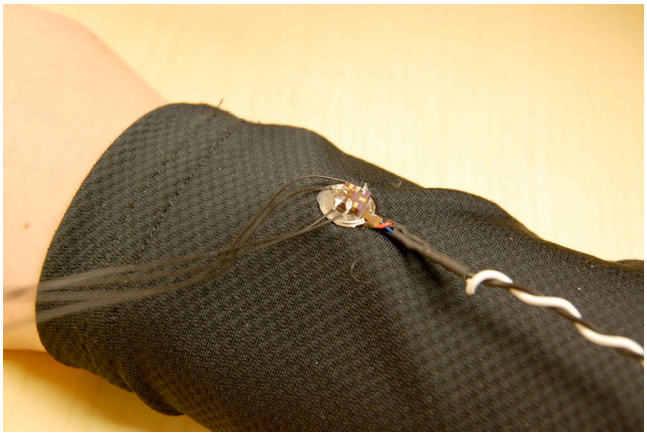

Figure 8: Experimental setup for identification of motor model parameters. A small accelerometer is attached to the back of the motor.

To identify our system's physical parameters, we disassembled a motor and directly measured the motor housing mass, the mass of the rotating part, and the radial location of its center of gravity. We also directly measured the mass of the cap. For the purposes of our model, the combined motor housing, rotating part, and cap mass is 1.5 g, the mass of the rotating part itself is 0.3 g, and the radial location of the center of gravity is 1.5 mm. Because the spring and damping constants represent composite materials, we avoided direct measurement and used iterative empirical tuning to make the model's behavior match the response of the physical system.

Next, we characterized the motor's torque constant and the frictional torque inside the motor. In order to do this, we needed to consider the electrical equation that represents our system:

$$V = Ri + L\dot{i} + k_e\dot{\theta} \tag{14}$$

Here, V is the potential difference across the motor's leads, R is the resistance of the motor coil, L is its inductance, and k_e is the motor's back-EMF constant. At steady-state, this equation simplifies to four measurable quantities: if we know the current, the potential difference across the motor, the motor resistance, and the angular velocity, we can determine the back-EMF constant. When this constant is calculated in volts per radians per second, it exactly equals the motor's torque constant in newtons per amp, which we need to know for accurate simulation of this system. Note that the shaftless motor's angular velocity $\dot{\theta}$ is not directly observable, but we know that it is the same as the oscillatory frequency ω of the housing's accelerations in radians per second.

To determine the back-EMF constant, we mounted an ADXL210E MEMS-based accelerometer directly to the back of one of the motors, as shown in Figure 8. This actuator was then attached to the fabric of the forearm of the Under Armour sleeve as it was being worn by a volunteer. We performed tests for steady-state currents ranging from zero to forty milliamps, recording potential difference V and acceleration frequency ω. Motor vibration frequency was found to vary from 86 Hz to 150 Hz, increasing with higher current levels. During this testing, we found that the resistance of the motor varies with angular position. Examination of a disassembled motor revealed that the motor brushes come into contact with two of six conductive plates on the rotating coil. The resistance between pairs of these plates is either 63 Ω or 33 Ω, depending on their locations. We accounted for this angular dependence by weighting these values appropriately and arrived at an average resistance of 44 Ω. From a set of forty steady-state experiments, we found the average back-EMF constant to be 0.00037 Vs.

The above mentioned experimental data can also be used to characterize the motor's frictional torque. At steady-state, equation (11) reduces so that τ_f equals $k_t i$. For every current i, we plotted this quantity τ_f versus ω. This plot supports the idea that this motor has some static friction that it must overcome before motion begins. Once static friction has been overcome ($\tau_{f,s} = 7.659 \times 10^{-6}$ Nm), τ_f takes the form of a positively-sloped line with a negative y-intercept:

$$\tau_f = (5.505 \times 10^{-8}\ \text{Nms})\omega - (7.5321 \times 10^{-6}\ \text{Nm}) \tag{15}$$

This behavior resembles viscous friction in that τ_f increases with increasing ω, but the fact that the linear fit has a negative y-intercept confirms the need for an empirical definition. To capture the widest range of frequencies possible, we used stepped current tests to capture hysteresis effects. For example, in one test, we commanded currents of 40 mA, 25 mA, 20 mA, and 15 mA in continuous ten second intervals. Because it is difficult to produce very low-frequency (<25 Hz) accelerations with our vibration motors, we assumed a horizontal line between the lowest measured frequency and its y-axis intercept ($\tau_f = 4.625 \times 10^{-6}$ Nm). In our Matlab model, the symmetric friction behavior takes the form of if-then statements. For every time step, our simulation uses the previous value of $\dot{\theta}$ to determine the present value of τ_f.

Finally, with all physical and electrical parameters defined, we correlated our model to experimental data. Using several different data sets, we tuned the spring and damping constants. We compared the frequencies, amplitudes, and magnitudes of motor housing and model-generated accelerations. The damping constants in the x- and y-directions are both equal to 1 Ns/m, while the spring constants in the x- and y-directions equal 2850 N/m and 3650 N/m, respectively.

7 Conclusion

This work explores the use of graded, spatially distributed vibrotactile feedback to assist in motor rehabilitation for apraxic stroke patients. To do this we have developed a VR-based wearable interface that can provide a combination of graphical and tactile feedback to the user. A magnetic motion capture system is used to track the user's arm; at each instant in time, our system converts the magnetic sensor data into the upper-limb joint angles, including four degrees of freedom. These angles are then compared with a desired arm pose, and our tactile feedback algorithms calculate an appropriate tactor activation pattern. To facilitate high performance control of our shaftless eccentric mass motors, we developed a dynamic model that matches experimental measurements of our tactile actuator's high frequency accelerations.

In future work, we plan to use the tactor's dynamic model to better shape our drive signals, in order to obtain the desired level of acceleration output from the actuator. The next step will be to undertake human subject testing on healthy subjects as well as apraxic stroke patients, in collaboration with the Moss Rehabilitation Research Institute in Philadelphia. Meanwhile, we are also committed to the development of novel and modular actuators to convey naturalistic contact sensations.

8 Acknowledgements

The authors wish to thank the members of the Penn Haptics Group. This work was supported by the University of Pennnsylvania and the National Science Foundation (IIS-0915560).

References

[1] American Heart Association. *Heart Disease and Stroke Statistics-2008 Update*, Dallas, Texas, 2008.

[2] P. Bach-y-Rita. Tactile sensory substitution studies. *Annals of the New York Academy of Science*, 1013:83–91, January 2006.

[3] K. Bark, J. Wheeler, G. Lee, J. Savall, and M. Cutkosky. A wearable skin stretch device for haptic feedback. In *Proc. IEEE World Haptics Conference*, pages 464–469, 2009.

[4] A. Bloomfield and N. I. Badler. Virtual Training via Vibrotactile Arrays. *Presence: Teleoperators and Virtual Environments*, 17(2):103–120, 2008.

[5] L. J. Buxbaum and H. B. Coslett. Limb Apraxia. In *New Encyclopedia of Neuroscience, L. Squire (Ed.)*, Amsterdam, 2008.

[6] A. Cassinelli, C. Reynolds, and M. Ishikawa. Augmenting spatial awareness with haptic radar. *Wearable Computers, 2006 10th IEEE International Symposium on*, pages 61–64, Oct. 2006.

[7] P. T. Chua, R. Crivella, B. Daly, N. Hu, R. Schaaf, D. Ventura, T. Camill, J. Hodgins, and R. Pausch. Training for physical tasks in virtual environments. In *Proc. IEEE Virtual Reality Conference*, pages 87–94, 2003.

[8] F. A. Geldard and C. E. Sherrick. The cutaneous "rabbit": a perceptual illusion. *Science*, 178(57):178–179, October 1972.

[9] B. T. Gleeson, S. K. Horschel, and W. R. Provancher. Communication of direction through lateral skin stretch at the fingertip. In *Proc. IEEE World Haptics Conference*, pages 172–177, 2009.

[10] M. K. Holden. Virtual environments for motor rehabilitation: Review. *CyberPsychology and Behavior*, 8(3):187–211, 2005.

[11] P. Kapur, S. Premakumar, S. A. Jax, L. J. Buxbaum, A. M. Dawson, and K. J. Kuchenbecker. Vibrotactile feedback system for intuitive upper-limb rehabilitation. In *Proc. IEEE World Haptics Conference*, pages 621–622, 2009.

[12] H. Krebs, N. Hogan, M. Aisen, and B. Volpe. Robot-aided neurorehabilitation. *IEEE Transactions on Rehabilitation Engineering*, 6(1):75–87, March 1998.

[13] G. Kwakkel, B. J. Kollen, and H. I. Krebs. Effects of Robot-Assisted Therapy on Upper Limb Recovery After Stroke: A Systematic Review. *Neurorehabilitation and Neural Repair*, 22(2):111–121, 2008.

[14] J. Lieberman and C. Breazeal. TIKL: development of a wearable vibrotactile feedback suit for improved human motor learning. *IEEE Transactions on Robotics*, 23(5):919–926, 2007.

[15] R. W. Lindeman, J. N. Templeman, J. L. Sibert, and J. R. Cutler. Handling of virtual contact in immersive virtual environments: beyond visuals. *Virtual Reality*, 6(3):130–139, 2002.

[16] F. Raab, E. Blood, T. Steiner, and H. Jones. Magnetic position and orientation tracking system. *IEEE Transactions on Aerospace and Electronic Systems*, AES-15(5):709–718, Sept. 1979.

[17] R. Riener, T. Nef, and G. Colombo. Robot-aided Neurorehabilitation for the Upper Extremities. *Medical and Biological Engineering and Computing*, 43:2–10, Jan. 2005.

[18] H. R.W. Lindeman, Y.Yanagida and K. Hosaka. Wearable Vibrotactile Systems for Virtual Contact and Information Display. In *Virtual Reality*, volume 9, pages 203–213, 2006.

[19] G. Slabaugh. *Computing Euler angles from a rotation matrix*. Technical Report, http://www.gregslabaugh.name/publications, 1999.

[20] R. Tadakuma and R. D. Howe. A whole-arm tactile display system. *Proc. IEEE World Haptics Conference*, 0:446–451, 2009.

[21] G. Welch and E. Foxlin. Motion tracking: No silver bullet, but a respectable arsenal. *IEEE Computer Graphics and Applications*, 22(6):24–38, 2002.

[22] H. Yano, T. Ogi, and M. Hirose. Development of haptic suit for whole human body using vibrators. *Transactions of the Virtual Reality Society of Japan*, 3(3):141–148, 1998.